Entanglement based tomography to probe new macroscopic forces

Barker, Peter F.; Bose, Sougato; Marshman, Ryan J.; Mazumdar, Anupam

Published in:
Physical Review D

DOI:
10.1103/PhysRevD.106.L041901

Publication date:
2022

Letter

Entanglement based tomography to probe new macroscopic forces

Peter F. Barker,[1] Sougato Bose,[1] Ryan J. Marshman,[2] and Anupam Mazumdar[3]

[1]*Department of Physics and Astronomy, University College London, Gower Street, WC1E 6BT London, United Kingdom*

[2]*Centre for Quantum Computation and Communication Technology, School of Mathematics and Physics, University of Queensland, Brisbane, Queensland 4072, Australia*

[3]*Van Swinderen Institute, University of Groningen, 9747 AG Groningen, Netherlands*

(Received 18 March 2022; accepted 28 July 2022; published 15 August 2022)

Quantum entanglement provides a novel way to test short distance physics in the nonrelativistic regime. We will provide a protocol to *potentially* test new physics by bringing two charged massive particle interferometers adjacent to each other. Being charged, the two superpositions will be entangled via electromagnetic interactions mediated by the photons, including the Coulomb and the Casimir-Polder potential. We will bring a method of *entanglement based tomography* to seek time evolution of very small entanglement phases to probe new physical effects mediated by *hitherto unknown macroscopic force* which might be responsible for entangling the two charged superpositions modeled by the Yukawa type potential. We will be able to constrain the Yukawa couplings $\alpha \geq 10^{-35}$ for $r \geq 10^{-6}$ m for new physics occurring in the electromagnetic sector, and in the gravitational potential $\alpha_g \geq 10^{-8}$ for $r \geq 10^{-6}$ m. Furthermore, our protocol can also constrain the axionlike particle mass and coupling, which is complimentary to the existing experimental bounds.

DOI: 10.1103/PhysRevD.106.L041901

One critical observation which parts from the classical world is the notion of quantum entanglement [1,2]. The latter provides the evidence of quantum correlation which a classical world cannot replicate. In particular, it is known that a classical interaction cannot entangle the two quantum systems (if they were not entangled to begin with) [3]. Since all the known Standard Model (SM) interactions and mediators are quantum in nature, *entanglement* formation becomes inevitable. The SM interactions are fairly well constrained by the collider [4], noncollider [5], the electron-dipole-moment (EDM) [6] experiments. However, there are consistent efforts in constraining weakly coupled bosons such as axionlike particle, Majorons, or light dark matter searches [7,8]. Given these advancements it is now paramount to seek a complimentary avenue to test new physics in the infrared (IR) and in a nonrelativistic (NR) limit.

The aim of this paper will be to provide a simple quantum-information lead *entanglement* protocol to confirm the SM interactions and to probe new physics in the particle physics and gravitational sectors. Very light and weakly coupled bosons could couple to the SM degrees of freedom, such as the axionlike particle, Kaluza-Klein modes from the extra dimensions, and hidden sector photon [5,7–10]. Axions with varied mass range are also expected in string theory [11], which provide a significant motivation to look for these light bosons experimentally. In the NR limit such corrections will generically yield Yukawa modifications to the potential mediated by these light bosons either at the tree or at the loop level [9]. Similarly, the quantum nature of the graviton within general relativity (GR) and beyond GR also tend to modify the gravitational potential which can be tested via *entanglement witness* [12–15].

In this paper, we will probe the nature of beyond the SM physics and the gravitational sector by witnessing the quantum entanglement between the two charged massive particle interferometers. Specifically, we will assume the interferometers induce a spatial superposition of size Δx. For details about explicit schemes of the sorts of interferometers considered, see Refs. [12,16,17].

To model this, we take an electronic spin in a host crystal, with a spin-spatial state coupling allowing us to measure the entanglement. We will assume a nitrogen-vacancy (NV) centre spin in a diamond nano/microcrystal, although qualitatively our results and analysis will hold for similar materials. We will further assume that the nanocrystal can be electrically charged. If we bring another such quantum superposition of a charged nanocrystal and keep them apart by a distance d, then the two nanocrystals will be entangled

via the exchange of a virtual photon (Coulomb), via the vacuum induced dipole-dipole type interactions mediated by the two photon exchange giving rise to the Casimir-Polder (CP) potential [18,19], and any additional particle-particle interactions which may occur. Since, at sufficiently short distances both the contributions will dominate the electromagnetic (EM) interactions, we study how to disentangle or mitigate the EM induced entanglement to probe new macroscopic forces in the EM sector and in the graitational sector.

In this paper, we will show that there exists parameter regions, where we can cancel the entanglement phase due to the Coulomb and the CP potential, and probe the configuration where the net entanglement phase due to the EM induced interactions vanishes (when $\Delta\phi_{em} = 2n\pi$, for $n = 0, 1, 2\cdots$). We will then show how by studying the entanglement entropy in the bipartite system, namely the von-Neumann entropy, we can probe for unknown force of nature in the IR. To detect a new force, we consider that the resulting particle-particle interactions produce different quantum correlations, which are captured by the time evolution of the *entanglement entropy*, i.e., *entanglement based tomography*. In general, we will describe this new force by a Yukawa potential without going into the details of model building.

Let us consider a setup where we have two charged nanocrystals, with an embedded, addressable spin, we will assume that they have the same mass m with a radius $R = (3m/4\pi\rho)^{1/3}$ where $\rho = 3.5 \times 10^3$ kgm^{-3} is the density of the nanocrystals, similar to that of the diamond, see Fig. 1. Each mass, labeled a and b, will be assumed to have a net charge $(q_a e, q_b e)$ where $q_i \in \mathbb{Z}$ and e is the charge of an electron. The interactions are expected to be in the IR and are thus limited to EM, gravitational and the unknown interactions mediated by beyond SM quanta. Since the nanocrystals have diamagnetic properties, typical for a diamond, there will be a CP potential on top of the Coulomb interaction. These will be the dominant EM interactions the crystals will face at relatively short distances, but still in the IR. The known potentials are

$$U_{cp}(x) = -\frac{23\hbar c}{4\pi}\frac{\epsilon - 1}{\epsilon + 2}\frac{R^6}{(x - 2R)^7} \tag{1}$$

$$U_c(x) = \frac{e^2}{4\pi\varepsilon_0}\frac{q_a q_b}{x} \tag{2}$$

where ϵ is the diamagnetic susceptibility. We consider the masses to be placed in a spatial superposition of size Δx in the parallel arrangement as shown in Fig. 1. For this configuration of masses, the joint quantum state of the spins $|\Psi(0)\rangle = \frac{1}{2}(|\uparrow,\uparrow\rangle + |\downarrow,\downarrow\rangle + |\uparrow,\downarrow\rangle + |\downarrow,\uparrow\rangle)$ will evolve to [12,13][1]:

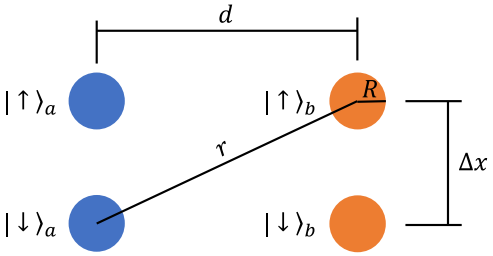

FIG. 1. Configuration where the two spatial superpositions with the splitting Δx are kept parallel to each other separated by a distance r, d. The two spin states have been shown, the radius of the spherical nanocrystal is R.

$$|\Psi(t)\rangle = \frac{1}{2}[|\uparrow,\uparrow\rangle + |\downarrow,\downarrow\rangle + e^{i\Delta\phi(d,r)}(|\uparrow,\downarrow\rangle + |\downarrow,\uparrow\rangle)]$$

where the phase ϕ is determined by the interaction considered: $\phi_i(x) = (t/\hbar)U_i(x)$, see [15,16], and is a function of the particle-particle distance d between the $|\uparrow\rangle_a$ and $|\uparrow\rangle_b$ states (which is the same as that for the joint state $|\downarrow,\downarrow\rangle$) and $\Delta\phi(d,r) = \phi(r) - \phi(d)$ where $r = \sqrt{d^2 + \Delta x^2}$ is the particle-particle distance for the joint states $|\uparrow,\downarrow\rangle$ (and equivalently $|\downarrow,\uparrow\rangle$). As such, there is only one important phase $\Delta\phi(d,\Delta x)$, which dictates whether or not the masses are entangled, which is why this arrangement is preferred. Further to these potentials, we will consider as an example of the Yukawa potential where we will constrain (α,λ), see [9,10].

$$U_Y(x) = \alpha e^{-x/\lambda}/x, \tag{3}$$

α dictates the interaction strength of the new physics and λ determines the effective range of the interaction, or related to the Compton wavelength $\lambda \sim 1/m_*$, where m_* denotes the particle mass which interacts with the EM photons. We will now discuss how, by carefully selecting the experimental parameters, we might hope to detect new close range forces and the modifications to these by eliminating the competing effects of the Coulomb and the CP interactions. To determine the parameter space in which

[1]The analogous system of quantum spatial superposition but with the neutral masses has been considered in Refs. [12,13]. The details of the entanglement phase evolution can be found in Refs. [12,13,20]. In these papers, the quantum nature of the graviton (spin-2 and spin-0 components of the quantum nature of graviton was responsible for entangling the two superpositions, see for a quantum field theory description [13,15]. Here, instead, we consider the quantum nature of the photon to entangle the two charged nanocrystals. Even the vacuum induced dipole-dipole interaction which gives rise to CP potential is being mediated by the virtual exchange of the photons [19].

the Coulomb and the *CP* interactions cancel, we will consider the entanglement phase due to each:

$$\Delta\phi_c = \frac{t}{\hbar}\frac{e^2}{4\pi\varepsilon_0}\left(\frac{q_a q_b}{r} - \frac{q_a q_b}{d}\right),$$
$$\Delta\phi_{cp} = -\frac{t}{\hbar}\frac{23\hbar c}{4\pi}\frac{\epsilon-1}{\epsilon+2}\left(\frac{R^6}{(r-2R)^7} - \frac{R^6}{(d-2R)^7}\right). \quad (4)$$

Thus, we require $\Delta\phi_c(d,r) = -\Delta\phi_{cp}(d,r)$. To consider a general situation, we use the parametrization; $\Delta x = \beta d$, $r = \sqrt{1+\beta}d$. This constrains

$$d = \left(\frac{\sqrt{1+\beta} - (1+\beta)^{-3}}{\sqrt{1+\beta}-1}\frac{23\hbar c\varepsilon_0}{e^2}\frac{\epsilon-1}{\epsilon+2}\frac{1}{q_a q_b}\right)^{1/6} R. \quad (5)$$

These results suggest that there are no solutions when $\text{sign}(q_a) \neq \text{sign}(q_b)$ as this leads to a complex valued d. The ability to detect a close range interaction within this regime will then be determined by the parameter stability, and the certainty from one run to the next. There is however a significant issue of the acceleration induced by the *CP* and the Coulomb interactions.

The two accelerations fail to cancel one another out, and leave a significant residual acceleration, which is only made larger by increasing the charges of the masses (q_a and q_b). This poses a strong limiting factor without some further mitigation strategy, which is what we will now present.

Now, we will present the analysis of the experimental configuration where we optimize the separation between the two superpositions involved, such that the *CP* and the Coulomb forces cancel. So that we are no longer optimizing over both the average distance d and Δx. The two EM forces are given by; $F_{cp}(x) = -(161\hbar c/4\pi)(\epsilon - 1/\epsilon + 2)R^6/(x-2R)^8$, and $F_c(x) = (e^2/4\pi\varepsilon_0)(q_a q_b/x^2)$. We can eliminate the net EM forces at a single distance d, which gives $F_{cp}(d) = -F_c(d)$. Setting $d = nR$ gives:

$$\frac{n^2}{(n-2)^8} = \frac{4\pi}{161\hbar c}\frac{\epsilon+2}{\epsilon-1}\frac{q_a q_b e^2}{4\pi\varepsilon_0}, \quad (6)$$

which gives $d \sim 6R$, for $q_a = q_b = 1$, $d \sim 4R$, for $q_a = q_b = 10$, and $d \sim 3R$, for $q_a = q_b = 100$.

This limits the charges to be, $q \lesssim \mathcal{O}(10)$. To allow a significant separation between the two nanocrystals, we will need to move into the regime where the forces only *approximately* cancel. To do this, we would set the minimum distance between the masses, d, to be such that the force between them cancels. The superposition size Δx can then be increased until the force between the distant states (each at a distance of r from one another) becomes significant. We will again use $d = nR$ to represent the exact

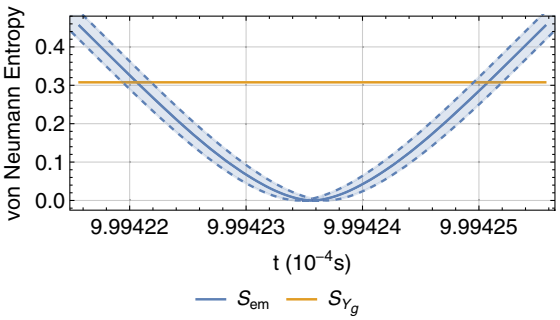

FIG. 2. von Neumann entropy with respect to time for all the interactions. The shaded region shows the uncertainty in the experimental parameters where the EM induced entanglement is used as a baseline. Here we have taken $R = 10^{-4}$ m, $\alpha_g = 0.01$, $\lambda = 10^{-3}$.

distance for which the forces cancel, and write $r = nR + r'$. The residual force is then

$$F_{\text{net}} = \left(\frac{161\hbar c}{4\pi}\frac{\epsilon-1}{\epsilon+2}\frac{8}{(n-2)^9} - \frac{e^2 q_a q_b}{4\pi\varepsilon_0}\frac{2}{n^3}\right)\frac{r'}{R^3} \quad (7)$$

Therefore, for example, when we take $q_a = q_b = 1$, and $n = 6$, we obtain $F_{\text{net}} \sim 10^{-29} r'/R^3$. This suggests that, depending on the tolerable force, even $r' \leq R$ could be possible. In this case, the superposition size is $\Delta x = ((nR + r')^2 - n^2R^2)^{1/2}$. For the purpose of illustration and in the remainder of the paper, and specifically for Figs. 2,3,5, we will take these optimized parameters,

$$d = 6R, \qquad r = 7R, \qquad \Delta x \approx 3.6R, \qquad q_1 = q_2 = 1. \quad (8)$$

We consider $R \in \{10^{-4}\text{ m}, 10^{-5}\text{ m}, 10^{-6}\text{ m}\}$, equivalently $m \in \{10^{-8}\text{ kg}, 10^{-11}\text{ kg}, 10^{-14}\text{ kg}\}$. It is, however, known that for a given mass m, the graviton vacuum gets displaced and this corresponds to the number of excited gravitons around the Minkowski vacuum which can be estimated by the Bekenstein's entropy [21]: $N_g = S_{\text{BEK}} \sim (m/M_p)^2$ [22]. For $m \sim 10^{-8}$ kg, it is actually $N_g \sim 1$, and for lighter mass $N_g \ll 1$. It appears that $N_g \sim \mathcal{O}(1)$ might dictate this subtle distinction between one graviton excitation with many graviton excitations in the vacuum. Here we have kept all our masses below the Planck mass, i.e., $m \leq 10^{-8}$ kg.

We will now consider a novel strategy to mitigate the EM induced phase through the tomography, i.e., experimental timing. Specifically, given the total EM-induced entanglement phase is $\Delta\phi_{em} = \Delta\phi_c + \Delta\phi_{cp}$, and provided the experimental parameters (m, t, d and Δx) are tuned sufficiently well, then ensuring

$$\Delta\phi_{em} = \Delta\phi_c + \Delta\phi_{cp} = 2\pi n \quad (9)$$

where $n \in \mathbb{Z}$ will remove any EM signal, leaving only the discovery potential for the other macroscopic forces beyond the SM.

This can be achieved by choosing an appropriate interaction time. If we are constraining the Yukawa potential, then by using our set-up we can utilize the force canceling region to enable a relative stable particle-particle interaction. That is, little or no deflection of the masses due to their EM interactions throughout the interferometry process. This can be seen in Fig. (2), where the entanglement entropy induced by the EM interaction between the two sub-systems vanishes, while the other interactions do not vanish at a specific point. Indeed, we have chosen a small snap-shot of time for the purpose of illustration, we can indeed take a larger time evolution. Just as an example, we have shown here the entanglement entropy for the gravitational induced Yukawa potential between the two systems do not vanish at that specific time. The shaded region in the EM induced entanglement denotes the uncertainties in the Coulomb and CP potential due to uncertainties in the experimental parameters, as discussed below.

The EM induced entanglement phases per unit time are given by:

$$\frac{\Delta\phi_c}{t} = \frac{1}{\hbar}\frac{e^2}{4\pi\epsilon_0}\left(\frac{q_a q_b}{r} - \frac{q_a q_b}{d}\right) \sim (5\times 10^4/R)\ \text{rad}\,\text{s}^{-1}$$
$$\frac{\Delta\phi_{CP}}{t} = \frac{1}{\hbar}\frac{23\hbar c}{4\pi}\frac{\epsilon-1}{\epsilon+2}\left(\frac{R^6}{(r-2R)^7} - \frac{R^6}{(d-2R)^7}\right)$$
$$\sim -(2\times 10^4/R)\ \text{rad}\,\text{s}^{-1}. \quad (10)$$

For any interaction time $t \gtrsim 10^{-4}R$ sec, the condition set out in Eq. (9) can be readily made true. We will consider the merit of two different scenarios of new physics.

(i) *Departure from the Coulomb and the CP potential:* We will consider the acceptable levels of uncertainties in the experimental parameters. To determine, approximately, we will consider the uncertainties by taylor expanding around their target values which suggests the Coulomb interaction will be

$$\Delta\phi_c(d,r) + \delta(\Delta\phi_c(d,r))$$
$$= \Delta\phi_c(d,r)(1+\delta t/t + \delta d/d + \delta r/r)$$
$$\equiv \Delta\phi_c(d,r)(1+3\tilde{\delta}), \quad (11)$$

where we have assumed every parameter has an equal relative error $\tilde{\delta}$ for simplicity. Similarly for the CP interaction, we obtain

$$\Delta\phi_{cp}(d,r) + \delta\Delta\phi_{cp}(d,r) \approx \Delta\phi_{cp}(d,r)(1+15\tilde{\delta}). \quad (12)$$

To ensure that the entanglement phases induced by the EM interactions does not remove that sourced by the Yukawa, $\delta\Delta\phi_{em} \ll \Delta\phi_Y$ and $\delta\Delta\phi_{em} \ll 1$, where $\Delta\phi_Y$ is the entanglement phase induced by the Yukawa term. Thus we will require $|\delta\Delta\phi_{em}| < 1$, which implies $\tilde{\delta}|(3\Delta\phi_c + 15\Delta\phi_{cp})| < 1$, or using Eq. (10): $\tilde{\delta} \leq 10^{-6}R/t$. Similarly, we must ensure that the gravitational interaction between the masses do not induce a coherence destroying noise. Given the gravitational entanglement phase is given by: $\Delta\phi_g = Gm^2t(r^{-1}-d^{-1})/\hbar$, to keep the variance below the unit phase will require $\delta\Delta\phi_g \approx \frac{40\pi^2\rho^2GR^5t}{189\hbar}\tilde{\delta} < 1$. Substituting known values and assuming diamond is used gives then gives the bound $\tilde{\delta} \lesssim 5\times 10^{-32}t^{-1}R^{-5}$. If we thus set $\tilde{\delta} \approx \min\{10^{-6}R/t, 10^{-32}t^{-1}R^{-5}\}$, then the Yukawa potential will be the dominant entangling signal, provided $|\Delta\Phi_y| \geq 1$. We then have a detectable Yukawa signal provided

$$\frac{\alpha t}{42\hbar R}\left(6e^{-\frac{7R}{\lambda}} - 7e^{-\frac{6R}{\lambda}}\right) \geq 1. \quad (13)$$

The Yukawa induced correction to the EM interaction is shown in Fig. 3. Its worth noting that this corresponds to the actual parameter uncertainties of: $\delta d = \min\{10^{-6}\times(R^2/t)\ \text{sec}\,\text{m}^{-1}, 10^{-32}\times t^{-1}R^{-4}\ \text{sec}\,\text{m}^5\}$, and $\delta t = \min\{10^{-6}\times R\ \text{sec}\,\text{m}^{-1}, 10^{-32}\times R^{-5}\ \text{sec}\,\text{m}^5\}$. This suggests that for a nanocrystal with a radius $R \sim 10^{-6}$ m we will need the precision in time for the measurement to be around 10^{-12} sec. This may pose a challenge but the recent advancements of keeping track of the frequency ratio measurements at 18-digit accuracy may be the way to track the time evolution of the entanglement [23].

(ii) *Axionlike particle detection:* We can also consider how our protocol may be sensitive to the axion modified Coulomb potential. Following previous analyses [24], assuming that the experiment involves distances larger than the Compton wavelength of the axion mass, the axion modified Coulomb potential is approximately given by: $U_{ac}(x) = U_c(x)(1+\frac{g^2\lambda^2\hbar^2}{\pi^2c^2x^4}e^{-x/\lambda})$ where g is the coupling strength and $\lambda = \frac{\hbar}{m_a c}$ is the Compton wavelength of the axion of mass m_a. The entanglement phase detectability requires $\Delta\phi_{ac} - \delta(\Delta\phi_{ac}) > \Delta\phi_c + \delta(\Delta\phi_c)$, which leads to

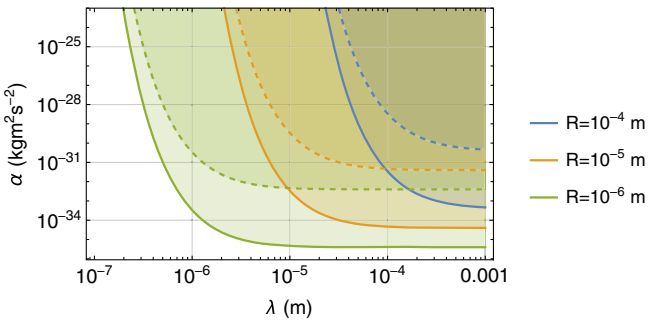

FIG. 3. $\alpha - \lambda$ plot showing the region in which the Yukawa potential dominates over the Casimir and Coulomb interactions for different values of R. The solid and dashed lines correspond to a total interaction time $t = 10^{-3}$, $t = 10^{-6}$ s, respectively.

$\Delta\phi_a > 2\delta(\Delta\phi_c)$. The latter condition gives the bound for a detectable g as

$$g \gtrsim \sqrt{6\frac{\pi^2 c^2}{\lambda^2\hbar^2}\left(\frac{1}{r}-\frac{1}{d}\right)\left(\frac{e^{-r/\lambda}}{r^5}-\frac{e^{-d/\lambda}}{d^5}\right)^{-1}\tilde{\delta}}. \quad (14)$$

We can see that the current observational bounds arising from [5,7,24–27] cover a large range of parameter space in g, m_a. We see that our current protocol will be sensitive to constrain masses below $m_a \leq 10^{-21}$ eV in future.

As such, taking the experimental set-up discussed above with $R = 10\ \mu$m suggests a the detectable coupling strength will be

$$g \gtrsim \frac{10^{35}}{\lambda}\left(2e^{-\frac{6}{10^{-5}\lambda}}-e^{-\frac{7}{10^{-5}\lambda}}\right)^{-1/2}\ \text{kg}^{-1} \quad (15)$$

as shown in Fig. 4.

(iii) *Departure from the Newtonian potential:* Following the above discussion, we can evaluate the entanglement phase as sourced by the quantum origin of the gravitational interaction [12,15,16] or as we will do here, a modification to the Newtonian potential. We can parametrize the departure from Newton's law by the Yukawa potential [28]:

$$U_{Y_g} = \frac{Gm^2}{r}(1+\alpha_g e^{-r/\lambda}) \quad (16)$$

In this case, a similar analysis as above, see Eq. (13) translates to a sensitivity in the effective gravitational coupling α_g given by Fig. 5. Note that the sensitivity to probe α_g in the vicinity of 10^{-5} m is far improved than what we have achieved in the torsion-balance experiments $\alpha_g \sim 10^{-3}$ in the μm range [29]. Figure 5 shows the experimental constraints from 2000 and 2007 of the same group, see [29].

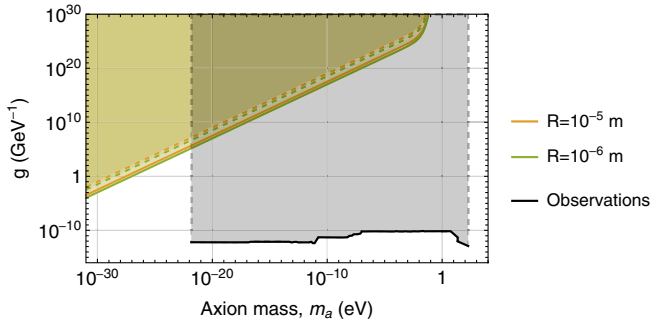

FIG. 4. Plot showing the region in which the axion modified Coulomb interaction is detectable using this entanglement based detection for the two configurations. The *observations* shown by the gray shaded region correspond to the combined results of many separate observations, such as CAST + SUMICO, cosmology, supernovae-1987A, electron-positron collider (LEP), OSCAR and PVLAS collaborations, compiled from the Refs. [5,7,24–27].

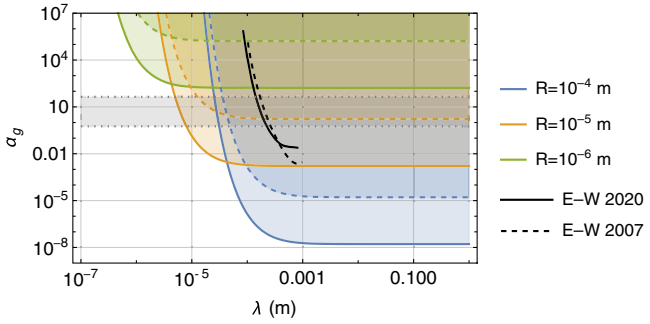

FIG. 5. $\alpha_g - \lambda$ plot showing the region in which the Yukawa modified Newtonian potential dominates over the Casimir and the Coulomb interactions for different values of R. The solid and dashed lines correspond to the total interaction time $t = 10^{-3}$, $t = 10^{-6}$ s, respectively. The two black lines (solid and dashed) correspond to the experimental results from the years 2007, 2020, see [29]. The horizontal gray area shows the region in which n-compact extra dimensions may be observable where $\alpha_g = 2n$. The typical range for $\alpha_g \leq 20$ from string theory compactification on a Calabi Yau manifold, see [30].

Large extra spatial dimensions [31,32] also modify the gravitational potential very similar to the Yukawa modification, Eq. (16), see [30]. The extra dimensions are compactified, which depends on the geometry of the compactification. However, different compactification will give rise to different α_g in Eq. (16). If n extra dimensions are compactified on a n-torus, then $\alpha_g = 2n$, when on n-spehere $\alpha_g = n+1$, and in the case of string theory compactification on a Calabi-Yau manifold it should be $\alpha_g \leq 20$ [30]. The corresponding $\alpha_g - \lambda$ plot is shown in Fig. 5 which suggests that our setup with entanglement tomography is capable of detecting modifications to the Newtonian potential for $\lambda \gtrsim 10^{-6}$ m, and eventually can probe certain aspects of string theory or the presence of large extra dimensions.[2]

To summarize, all the examples capture the importance of entanglement based tomography as a protocol to test new physics—whether it is in the EM sector or in the gravitational sector. Indeed, there are many challenges from creating charged superposition [34] in a levitated ion trap, see [35–40], to preparing and cooling the ground state of

[2]Similarly, we can also constrain the hidden sector photon, for which the modified Coulomb potential can be derived very similar to the modification to the gravitational potential [33], $V(r) = [e^2/(4\pi\epsilon_0 r)][1+\alpha e^{-m_{\gamma'}r}]$. Here $m_{\gamma'}$ is the mass of the hidden photon and $\sqrt{\alpha}$ designates the coupling between the hidden sector photon and the Standard Model photon, i.e., $(\sqrt{\alpha}/2)X_{\mu\nu}F^{\mu\nu}$. $X_{\mu\nu}$ denotes the hidden sector photon and $F_{\mu\nu}$ denotes the Standard Model photon, and $\mu\nu = 0, 1, 2, 3$. In this scenario we can constrain $m_{\gamma'} \leq 10^{-17}$ eV for $\alpha \geq 10^{-4}$. The current constraints on the hidden sector photon mostly arises from astrophysics, and they can constrain $m_{\gamma'} \sim \mathcal{O}(10^{-10}$–$10^{-15})$ eV, see [33].

the nanocrystal [41]. There will be constraints on the decoherence [42], but we expect the decoherence rates will be very similar to the case of the neutral crystal, as far as the blackbody and the atmospheric interactions are concerned for a micron size crystal with a mass of $\sim 10^{-17}$ Kg [20,43]. However, there are possible ways of mitigating EM induced decoherence by creating a Faraday cage, and also the gravity gradient and relative acceleration noise [44].

To conclude, the entanglement based tomography could potentially be a powerful protocol to detect new physics in the IR. One can apply this technique to probe modifications to GR including local [45] and nonlocal modifications of classical and quantum gravity [46–48]. In physics beyond the SM, we will be able to probe certain model dependent parameters case by case [8,9,27]. The last reference considered axion induced entanglement, however, not in the context of EM background effects arising from Coulomb and *CP*-induced entanglement.

In a model independent fashion the entanglement based tomography can constrain the Yukawa parameters $\alpha \geq 10^{-35}$ for $r \geq 10^{-6}$ m for the new forces, and a similar modification in the gravitational potential would yield constraining $\alpha_g \geq 10^{-8}$ for $r \geq 10^{-6}$ m, nearly five-orders of magnitude better than the current bounds arising from the classical torsion-balanced experiment [29]. In this way we can also place future constraints on the large extra compact dimensions. Furthermore, in the case of axionlike particle detection, we are sensitive to even smaller axion masses (smaller than the existing constraints from various astrophysical and cosmological observations), but not for small couplings, see Fig. 4. Nevertheless, entanglement tomography in conjunction with other datasets will be extremely helpful to probe axion masses below 10^{-21} eV, thereby probing both Yukawa type correction as well as more sophisticated potentials arising due to axionlike particles.

P. F. B. acknowledges funding from the EPSRC Grant No. EP/N031105/1 and the H2020-EU.1.2.1 TEQ project Grant agreement ID: 766900. S. B. acknowledges the EPSRC Grant No. EP/S000267/1, A. M. acknowledges (NWO) Grant No. 680-91-119 and R. J. M. was supported by the Australian Research Council (ARC) under the Centre of Excellence for Quantum Computation and Communication Technology (CE170100012).

[1] E. Schrödinger, Discussion of probability relations between separated systems, Proc. Cambridge Philos. Soc. **31**, 555 (1935).
[2] M. Horodecki, P. Horodecki, and R. Horodecki, Mixed-State Entanglement and Distillation: Is there a "Bound" Entanglement in Nature?, Phys. Rev. Lett. **80**, 5239 (1998).
[3] C. H. Bennett, D. P. DiVincenzo, J. A. Smolin, and W. K. Wootters, Mixed-state entanglement and quantum error correction, Phys. Rev. A **54**, 3824 (1996).
[4] P. A. Zyla *et al.* (Particle Data Group), Review of Particle Physics, Prog. Theor. Exp. Phys. **2020**, 083C01 (2020).
[5] J. Jaeckel and A. Ringwald, The low-energy frontier of particle physics, Annu. Rev. Nucl. Part. Sci. **60**, 405 (2010).
[6] T. E. Chupp, P. Fierlinger, M. J. Ramsey-Musolf, and J. T. Singh, Electric dipole moments of atoms, molecules, nuclei, and particles, Rev. Mod. Phys. **91**, 015001 (2019).
[7] R. Essig, J. A. Jaros, W. Wester, P. Hansson Adrian, S. Andreas, T. Averett, O. Baker, B. Batell, M. Battaglieri, J. Beacham *et al.*, Working group report: New light weakly coupled particles, arXiv:1311.0029.
[8] P. W. Graham, I. G. Irastorza, S. K. Lamoreaux, A. Lindner, and K. A. van Bibber, Experimental searches for the axion and axion-like particles, Annu. Rev. Nucl. Part. Sci. **65**, 485 (2015).
[9] J. E. Moody and Frank Wilczek, New macroscopic forces?, Phys. Rev. D **30**, 130 (1984).
[10] G. L. Klimchitskaya and V. M. Mostepanenko, Dark matter axions, non-Newtonian gravity and constraints on them from recent measurements of the Casimir force in the micrometer separation range, Universe **7**, 343 (2021); G. L. Klimchitskaya, Constraints on theoretical predictions beyond the standard model from the Casimir effect and some other tabletop physics, Universe **7**, 47 (2021).
[11] P. Svrcek and E. Witten, Axions in string theory, J. High Energy Phys. 06 (2006) 051.
[12] S. Bose, A. Mazumdar, G. W. Morley, H. Ulbricht, M. Toroš, M. Paternostro, A. A. Geraci, P. F. Barker, M. S. Kim, and G. Milburn, Spin Entanglement Witness for Quantum Gravity, Phys. Rev. Lett. **119**, 240401 (2017).
[13] R. J. Marshman, A. Mazumdar, and S. Bose, Locality and entanglement in table-top testing of the quantum nature of linearized gravity, Phys. Rev. A **101**, 052110 (2020).
[14] C. Marletto and V. Vedral, Gravitationally induced entanglement between two massive particles is sufficient evidence of quantum effects in gravity, Phys. Rev. Lett. **119**, 240402 (2017).
[15] S. Bose, A. Mazumdar, M. Schut, and M. Toroš, Mechanism for the quantum natured gravitons to entangle masses, Phys. Rev. D **105**, 106028 (2022).
[16] R. J. Marshman, A. Mazumdar, R. Folman, and S. Bose, Large splitting massive Schrödinger kittens, Phys. Rev. Research **4**, 023087 (2022).
[17] Y. Margalit, O. Dobkowski, Z. Zhou, O. Amit, Y. Japha, S. Moukouri, D. Rohrlich, A. Mazumdar, S. Bose, and C. Henkel *et al.*, Realization of a complete Stern-Gerlach

interferometer: Towards a test of quantum gravity, Sci. Adv. **7**, eabg2879 (2021).
[18] H. Casimir and D. Polder, The Influence of Retardation on the London-van der Waals Forces, Phys. Rev. **73**, 360 (1948).
[19] B. J. Holstein, Comment on ? The van der Waals interaction, Am. J. Phys. **69**, 1283 (2001).
[20] T. W. van de Kamp, R. J. Marshman, S. Bose, and A. Mazumdar, Quantum gravity witness via entanglement of masses: Casimir screening, Phys. Rev. A **102**, 062807 (2020).
[21] J. D. Bekenstein, Universal upper bound on the entropy-to-energy ratio for bounded systems, Phys. Rev. D **23**, 287 (1981).
[22] S. Bose, A. Mazumdar, and M. Toroš, Gravitons in a box, Phys. Rev. D **104**, 066019 (2021); Infrared scaling for a graviton condensate, arXiv:2110.04536.
[23] Boulder Atomic Clock Optical Network (BACON) Collaboration*, Frequency ratio measurements at 18-digit accuracy using an optical clock network, Nature (London) **591**, 564 (2021).
[24] S. Villalba-Chávez, A. Golub, and C. Müller, Axion-modified photon propagator, Coulomb potential, and Lamb shift, Phys. Rev. D **98**, 115008 (2018).
[25] S. Alekhin *et al.*, A facility to search for hidden particles at the CERN SPS: The SHiP physics case, Rep. Prog. Phys. **79**, 124201 (2016).
[26] M. Arik *et al.*, Search for Sub-eV Mass Solar Axions by the CERN Axion Solar Telescope with 3He Buffer Gas, Phys. Rev. Lett. **107**, 261302 (2011).
[27] A. Capolupo, G. Lambiase, A. Quaranta, and S. M. Giampaolo, Probing axion mediated fermion–fermion interaction by means of entanglement, Phys. Lett. B **804**, 135407 (2020).
[28] E. G. Adelberger, B. R. Heckel, and A. E. Nelson, Tests of the gravitational inverse square law, Annu. Rev. Nucl. Part. Sci. **53**, 77 (2003).
[29] J. G. Lee, E. G. Adelberger, T. S. Cook, S. M. Fleischer, and B. R. Heckel, New Test of the Gravitational $1/r^2$ Law at Separations Down to 52 μm, Phys. Rev. Lett. **124**, 101101 (2020).
[30] A. Kehagias and K. Sfetsos, Deviations from the $1/r^2$ Newton law due to extra dimensions, Phys. Lett. B **472**, 39 (2000).
[31] I. Antoniadis, S. Dimopoulos, and G. R. Dvali, Millimeter range forces in superstring theories with weak scale compactification, Nucl. Phys. **B516**, 70 (1998).
[32] N. Arkani-Hamed, S. Dimopoulos, and G. R. Dvali, The hierarchy problem and new dimensions at a millimeter, Phys. Lett. B **429**, 263 (1998).
[33] D. Kroff and P. C. Malta, Constraining hidden photons via atomic force microscope measurements and the Plimpton-Lawton experiment, Phys. Rev. D **102**, 095015 (2020).
[34] C. Monroe, D. M. Meekhof, B. E. King, and D. J. Wineland, A "Schrödinger Cat" Superposition State of an Atom, Science **272**, 1131 (1996); D. J. Wineland, Nobel lecture. Superposition, entanglement, and raising Schrödinger's cat, Rev. Mod. Phys. **85**, 1103 (2013).
[35] P. F. Barker, Doppler Cooling a Microsphere, Phys. Rev. Lett. **105**, 073002 (2010).
[36] T. W. Penny, A. Pontin, and P. F. Barker, Sympathetic cooling and squeezing of two co-levitated nanoparticles, arXiv:2111.03123.
[37] Z. Wei, H. Li, Y. Cao, C. Wu, J. Ren, Z. Hang, H. Chen, D. Zhang, and C. T. Chan, Spatially coherent surface resonance states derived from magnetic resonances, New J. Phys. **12**, 093020 (2010).
[38] O. Romero-Isart, A. C. Pflanzer, F. Blaser, R. Kaltenbaek, N. Kiesel, M. Aspelmeyer, and J. I. Cirac, Large Quantum Superpositions and Interference of Massive Nanometer-Sized Objects, Phys. Rev. Lett. **107**, 020405 (2011).
[39] T. Delord, P. Huillery, L. Nicolas, and G. Hétet, Spin-cooling of the motion of a trapped diamond, Nature (London) **580**, 56 (2020).
[40] J.-F. Hsu, P. Ji, C. W. Lewandowski, and B. D'Urso, Cooling the motion of diamond nanocrystals in a magneto-gravitational trap in high vacuum, Sci. Rep. **6**, 30125 (2016).
[41] U. Delic, M. Reisenbauer, K. Dare, D. Grass, V. Vuletić, N. Kiesel, and M. Aspelmeyer, Cooling of a levitated nanoparticle to the motional quantum ground state, Science **367**, 892 (2020); F. Tebbenjohanns, M. Frimmer, V. Jain, D. Windey, and L. Novotny, Motional Sideband Asymmetry of a Nanoparticle Optically Levitated in Free Space, Phys. Rev. Lett. **124**, 013603 (2020).
[42] O. Romero-Isart, Quantum superposition of massive objects and collapse models, Phys. Rev. A **84**, 052121 (2011); A. Bassi, K. Lochan, S. Satin, T. P. Singh, and H. Ulbricht, Models of wave-function collapse, underlying theories, and experimental tests, Rev. Mod. Phys. **85**, 471 (2013).
[43] J. Tilly, R. J. Marshman, A. Mazumdar, and S. Bose, Qudits for witnessing quantum-gravity-induced entanglement of masses under decoherence, Phys. Rev. A **104**, 052416 (2021); M. Schut, J. Tilly, R. J. Marshman, S. Bose, and A. Mazumdar, Improving resilience of quantum-gravity-induced entanglement of masses to decoherence using three superpositions, Phys. Rev. A **105**, 032411 (2022).
[44] M. Toroš, T. W. Van De Kamp, R. J. Marshman, M. S. Kim, A. Mazumdar, and S. Bose, Relative acceleration noise mitigation for nanocrystal matter-wave interferometry: Applications to entangling masses via quantum gravity, Phys. Rev. Research **3**, 023178 (2021).
[45] A. Addazi *et al.*, Quantum gravity phenomenology at the dawn of the multi-messenger era—A review, Prog. Part. Nucl. Phys. **125**, 103948 (2022).
[46] T. Biswas, E. Gerwick, T. Koivisto, and A. Mazumdar, Towards Singularity and Ghost Free Theories of Gravity, Phys. Rev. Lett. **108**, 031101 (2012); T. Biswas, A. Mazumdar, and W. Siegel, Bouncing universes in string-inspired gravity, J. Cosmol. Astropart. Phys. 03 (2006) 009.
[47] E. T. Tomboulis, Superrenormalizable gauge, and gravitational theories, arXiv:hep-th/9702146; L. Modesto, Super-renormalizable quantum gravity, Phys. Rev. D **86**, 044005 (2012).
[48] J. Edholm, A. S. Koshelev, and A. Mazumdar, Behavior of the Newtonian potential for ghost-free gravity and singularity-free gravity, Phys. Rev. D **94**, 104033 (2016).